Journal of Visualization, Vol. 7, No. 4 (2004) 291-298

Visualization of dilute hydrogen jet flame in air flow

Chinone, S.* and Fujisawa, N.*

* Department of Mechanical Engineering, Niigata University, 8050 Ikarashi 2, Niigata, 950-2181, Japan.

Received 27 March 2004
Revised 28 May 2004

Abstract : The structure of hydrogen jet flame diluted by CO_2 in air flow is studied by various visualization techniques, such as schlieren, direct photograph, tracer injection and reactive Mie scattering method, which allow understanding of the influence of CO_2 on the characteristics of the hydrogen jet flame. The experimental result indicates that the flame structure consists of laminar fuel jet and surrounding reaction zone near the nozzle exit. When the CO_2 fraction is increased, the width of the fuel jet grows and the reaction zone is reduced in size. These observations are further confirmed by quantitative measurements of temperature and velocity fields in the flame, which are evaluated by thermocouple and particle image velocimetry (PIV), respectively. These results indicate that the flame temperature is decreased and the flow rate of the fuel jet is increased by the influence of diluents, which are due to the reduced calorific value and larger density of fuel, respectively.

Keywords : Flow visualization, Diffusion flame, Hydrogen, PIV, Temperature, Velocity.

1. Introduction

The study of hydrogen flame is an important topic of interest both from the fundamental and the practical point of view in combustion engineering. When the hydrogen is introduced as a fuel into industrial burners, the emission of pollutants, such as COx, NOx, unburnt hydrocarbons and particulates can be kept to lower level than that of conventional fuels. Therefore, there are many research works on the fundamental characteristics of hydrogen flame, which covers the chemical reaction mechanism, the extinction of flame, the temperature and the species concentration in the flame (e.g., Aung et al. 1998). On the other hand, the effects of diluents on the NOx formation in the flame are investigated by Feese and Turns (1998), Barlow et al. (1999) and Rortveit et al. (2002). They observed the reduction of NOx emission in the flame by the influence of diluents, which suggests the effectiveness of the flue gas recirculation technique for reducing NOx.

In order to understand the physical and chemical mechanisms of combustion and flame structure, the flow visualization studies have been carried out, which cover the extent of chemical reaction zone, temperature, velocity and the species concentration etc. Moreover, lots of efforts have been paid to the development of visualization techniques for application to the combustion phenomenon (Roquemore and Katta 2000; Chung 2003). The most well-known methods of flame visualization are shadowgraph, schlieren and interferometry (Stella et al. 2000), which assist the interpretation of flame geometry representing the position of highest gradient of density or temperature in the flame. The direct photography (Eickhoff and Winandy 1991; Nishimura et al. 1999; Hargrave et al. 2001), the reactive Mie scattering (Chen and Roquemore 1986; Shioji et al. 1993) and the laser-induced fluorescence provide the information on temperature and species

concentration in the flame. Some of these visualization techniques are extended to quantitative measurements of temperature, velocity and fraction of reactants in flame using the image processing of the visualized images (Fiechtner et al. 2000; Kawanabe et al. 2000; Takagi et al., 2000; Watson et al. 2000 and Tomimatsu et al. 2003). However, there are very few studies on the structure of dilute hydrogen jet flame.

The purpose of the present study is to understand the structure of the dilute hydrogen jet flame in air flow using various visualization techniques, such as schlieren, direct photograph, tracer injection and reactive Mie scattering method. The special attention is placed on the influence of CO_2 fraction on the temperature and velocity fields of the flame, which are measured by thermocouple and PIV, respectively.

2. Experimental Apparatus and Procedure

2.1 Experimental Apparatus

The experimental apparatus is shown in Fig. 1(a). The hydrogen is mixed with CO_2 in the mixing chamber and supplied to the test section through the straight circular tube. The cross-sectional area of the test section is 120mm × 120mm and its height is 300mm, which is made of heat resisting glass to keep transparent for the purpose of observation. The dilute hydrogen diffusion flame is generated at the nozzle exit, which has the inner diameter D (=6mm). The tube length of the nozzle (=300mm) is long enough, so that the flow is fully developed in the pipe. The flow rate of each gas was measured by the volumetric flow meters located between the gas tank and the nozzle. The volumetric fraction of CO_2 in the mixture gas was varied in the range of 0 to 60%, while the total flow rate was set constant to produce the bulk velocity 0.4m/s at the nozzle exit to keep the flame in laminar state. In order to stabilize the flame oscillation, a uniform co-flow of air is provided in the test section, which is set at 0.3m/s in the present experiment.

2.2 Visualization of Flow Field

The structure of dilute hydrogen flame in air flow was visualized by four different visualization techniques, such as schlieren, direct photograph, tracer injection and reactive Mie scattering method.

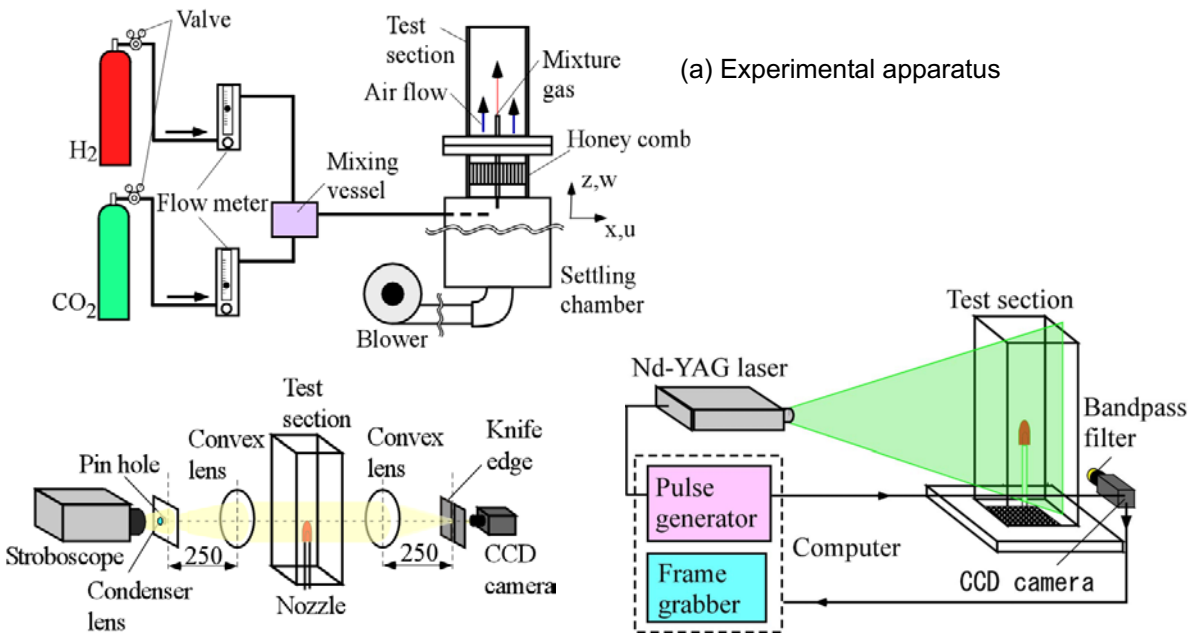

Fig. 1. Experimental arrangement.

The schlieren photograph provides the contours of density gradient, which is mostly generated by the temperature field and slightly by the density difference between the working gases. The optical arrangement is shown in Fig. 1(b), where the Xenon light from a stroboscope is used as a light source. The image is taken by a monochrome CCD camera having a spatial resolution 768× 494 pixels with 8 bits. The direct photograph is useful for understanding of chemical reaction zone in the flame. The luminosity of the flame is so weak that the flame image is taken by monochrome CCD camera with 12 bits having the spatial resolution 1280× 1028 pixels. The flow visualization by tracer injection method uses sphere particles of SiO_2 having a diameter of 2 μm . These tracers are supplied from the tank located upstream of the nozzle. The tank was oscillated using a vibrator to suspend the particles uniformly in the fuel flow. The reactive Mie scattering method allows the visualization of water vapor distribution in the flame. This technique provides the tracer particles of TiO_2 in the flame, where the vapor of $TiCl_4$ in the fuel flow reacts with the water vapor generated in the flame. Note that $TiCl_4$ (liquid) is supplied in the tank upstream of the nozzle to generate the $TiCl_4$ (vapor) in the fuel flow.

2.3 Measurement of temperature and velocity

The distributions of temperature and velocity in the flame were measured to understand the structure quantitatively. The temperature was measured pointwise by a thermocouple consisting of Pt-13%Rh wire of 0.3mm in diameter. Although the wires are uncoated, the probe remains unaffected by catalytic effects for several hours. The thermocouple signals were processed and time-averaged in a computer using an A-D converter. Note that the influence of radiation is corrected in reference to Sislian et al. (1988), however, the loss of heat transfer through the wire is found to be negligibly small. The uncertainty in the mean temperature measurement is estimated as 16K at 95% coverage, which is mostly due to the random error by flame unsteadiness 14K, the uncertainty in radiation correction 6K and the non-linearity of response curve 4K and others.

The velocity field is measured by PIV system, which is shown in Fig. 1(c). In the present experiment, the tracer particles of SiO_2 are supplied to the mixture gas at the tracer tank upstream of the fuel nozzle. The mean diameter of SiO_2 particles is about 2 μm. Note that the tracer tank was oscillated by a vibrator to suspend the particles in the mixture gas, similar to the visualization by tracer injection method. The tracer particles are illuminated by a light sheet from Nd: YAG laser of 30mJ and the images are captured by the monochrome CCD camera having spatial resolution 1018× 1008 pixels with 8 bits. The thickness of the light sheet was about 1mm. The double shutter function of the camera allows the imaging of sequential two images in a short time interval of 100 μs. Note that the bandpass filter of 532nm in central wavelength with 3nm bandwidth was placed in front of the CCD camera to remove the influence of flame noise. The target area of the images is 30mm× 30mm, so that the average pixel displacement of the particles between two images is about 5 pixels in the jet flow. The PIV processing was carried out using a direct cross-correlation algorithms with correlation window size of 31× 31pixels and search window size of 15× 15 pixels. The sub-pixel analysis was incorporated into the analysis to increase the accuracy of measurement. The uncertainty in velocity measurement is estimated to 3%. The details of uncertainty analysis can be found in Fujisawa et al. (2003).

3. Results and Discussion

3.1 Visualization of flame

Figure 2 shows schilieren photographs of the flame. The pictures are taken at volumetric concentration of 0, 20, 40 and 60% of CO_2 in the flame. Note that the blow-off limit of the flame was found to be CO_2=80% in the present experimental condition. All the pictures indicate that the flame boundaries are created on both sides of the flame and they are in laminar state. It is found that the flame boundary moves toward the center of the flame with an increase in CO_2 fraction. Therefore, the flame temperature is expected to decrease with an increase in CO_2 fraction.

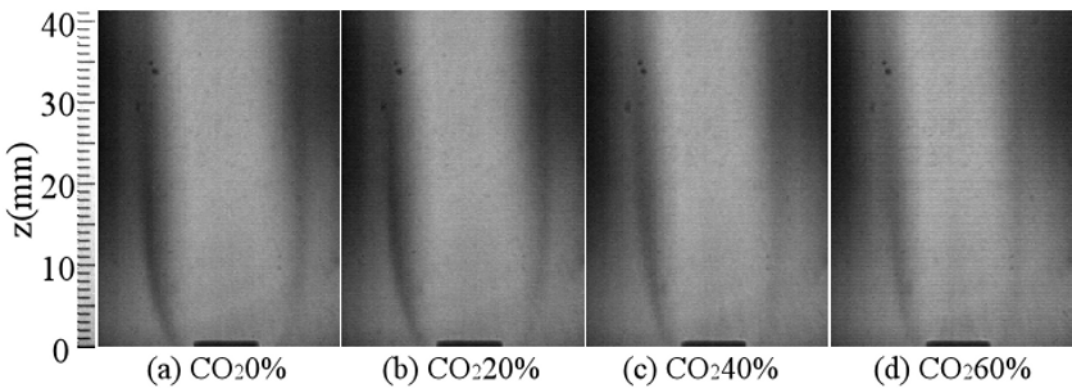

Fig. 2. Schlieren photographs.

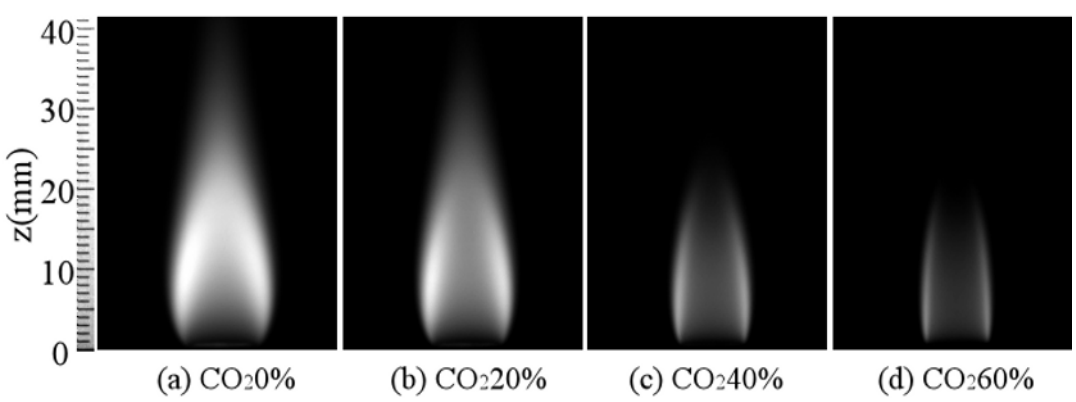

Fig. 3. Direct photographs.

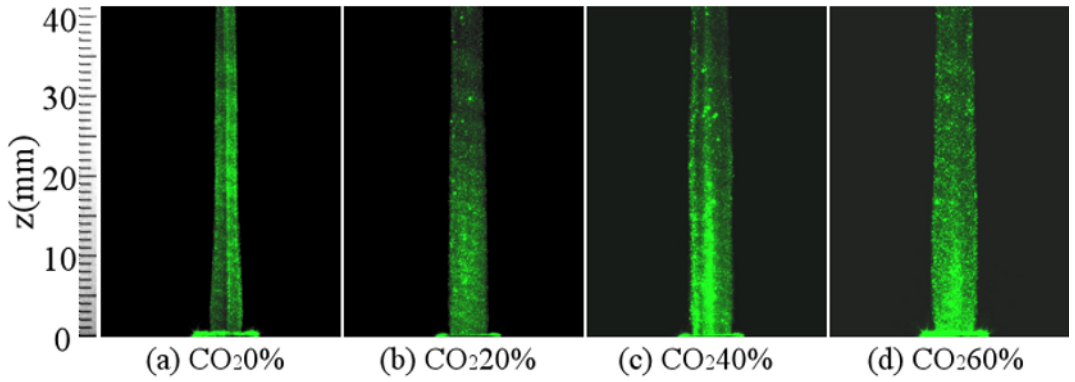

Fig. 4. Flow visualization by tracer injection method.

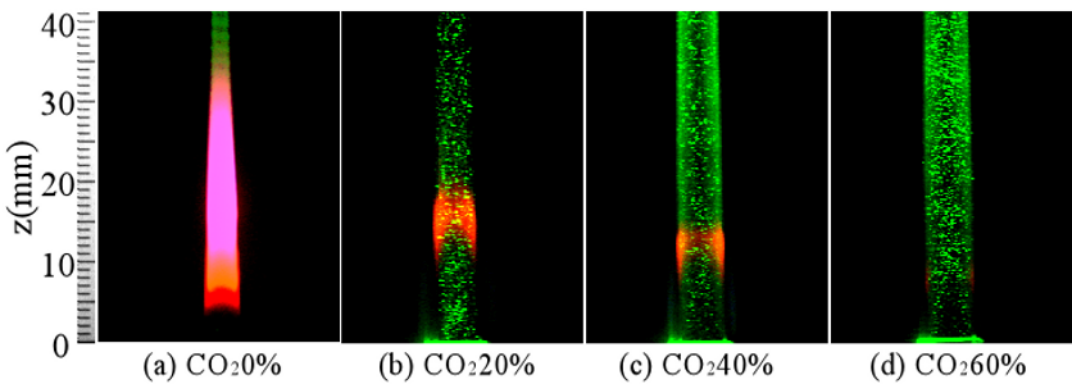

Fig. 5. Flow visualization by reactive Mie scattering method.

Figure 3 shows the flame visualizations by direct photograph, which are taken at various CO_2 fractions in the flame. The visualization pictures show the chemical reaction zone of the flame, which is formed around the nozzle exit. It is clearly seen that the area of reaction zone is decreased with an increase in CO_2 fraction, which corresponds to the inner movement of reaction front with an increase in CO_2 fraction.

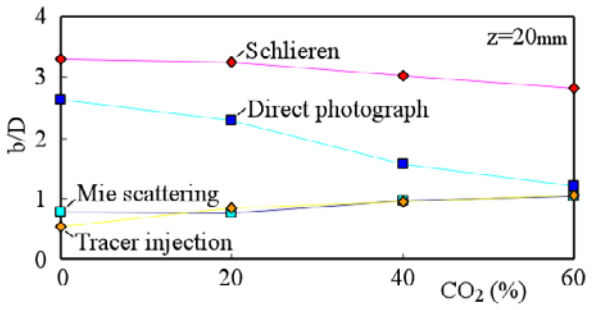

Fig. 6. Widths of flame and jet versus CO_2 fraction.

Figure 4 indicates the flow field visualized by the tracer injection method at various CO_2 fractions in the flame. The flow goes up along the flame axis straightly independent of the CO_2 fraction. Although the entrained fluid from the outside does not contain the tracers, the width of the jet grows with an increase in CO_2 fraction, which suggests an increase in flow rate of the jet entraining the surrounding air through the jet boundary. The smaller entrainment of the pure hydrogen flow is expected to be due to the smaller fluid density. With an increase in CO_2 concentration, the density of the jet flow increases and then the entrainment rate increases, which results in a growth of jet width.

Figure 5 shows the flow image visualized by reactive Mie scattering method at various fractions of CO_2 in the flame. They show the distributions of water vapor in the flame, which are generated from the reaction of hydrogen and oxygen in the air. Therefore, the reaction zone is formed around the shear layer extending from the nozzle exit and spread upward. With an increase in CO_2 fraction, the reaction zone grows laterally, which is similar to the flow visualization by tracer injection method in Fig. 4. Note that the green color indicates the TiO_2 particles and the red color may correspond to the reaction zone of $TiCl_4$ with the flame.

The widths of flame and jet are estimated from the visualization pictures to understand the effect of CO_2 quantitatively, which are shown in Fig. 6. Note that the width b is evaluated by image analysis of the intensity distribution along the line at z=20mm. It is clearly seen that the flame width obtained from the schlieren and direct photograph is decreased and the jet width obtained from the tracer injection and reactive Mie scattering method is increased, when the CO_2 fraction increases. However, there are quantitative differences between the results because of the different physical quantities of the flame. The chemical reaction zone (Mie scattering method) is decreased much faster than that of the density field of the flame (schlieren) with an increase in CO_2 fraction. On the other hand, the growth of jet flow by the tracer injection and Mie scattering method are in close agreement with each other except for the result at CO_2=0%, where the luminous flame is generated by the chemical reaction.

3.2 Measurement of temperature and velocity

Figures 7 and 8 show the horizontal and vertical distributions of temperature in the flame, respectively, which are measured by thermocouple. The horizontal temperature distributions (Fig. 6) are shown for the cases of CO_2 = 0 and 40% at three vertical positions z/D=0.8, 3.3 and 6.7 from the nozzle exit. Generally speaking, the temperatures of the dilute hydrogen flame are smaller than those of the pure hydrogen flame, which is due to the reduction in the gross calorific value of the mixture gas. This result agrees qualitatively with the schlieren visualization in Fig. 2. The temperature distribution at z/D=0.8 shows two peaks on both sides of the flame indicating the formation of flame front at the interface between the fuel and surrounding air. The positions of temperature peaks shift to the inner side of the flame with an increase in CO_2 concentration, indicating the inner shift of the fuel interface as observed in the direct photographs in Fig.3. Note that the image from direct photograph shows the line integral of the flame luminosity, which is different from the point measurement by thermocouple. With an increase in measurement position to z/D=3.3 and 6.7, the temperature peak moves to the center of the flame, which indicates the merging of flame front at the flame center.

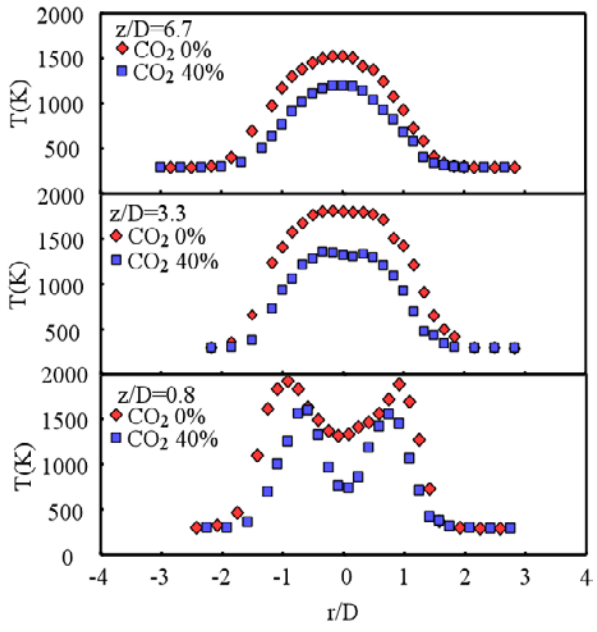

Fig. 7. Temperature distributions.

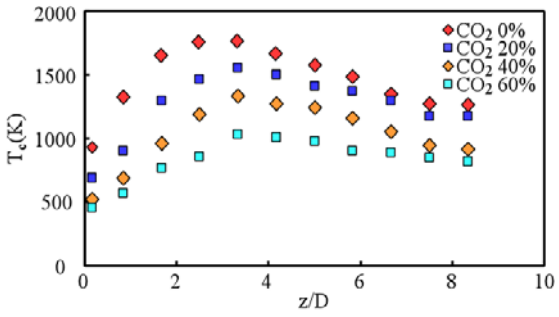

Fig. 8. Variations of temperatures along flame axis.

The vertical variations of temperature along the flame axis are shown in Fig. 8 at various CO_2 fractions. It is clearly seen that the highest temperatures are observed by pure hydrogen and they decrease gradually with an increase in CO_2 fraction. All temperature distributions show a sudden increase near the nozzle exit up to z/D=3-4, which corresponds to the reaction zone of the flame. This is followed by the gradual decrease in temperature due to the reduction in fuel concentration with an increase in vertical position z/D. Although the temperatures decrease gradually with an increase in CO_2 fraction, the shape of the temperature distributions is similar to that of the pure hydrogen.

Figures 9(a), (b) indicate the horizontal velocity distributions of pure and dilute hydrogen flames, respectively, which are measured by PIV, where w is the vertical velocity and W_0 is the bulk velocity obtained from the flow meters. Although the velocity distributions near the nozzle exit show peaks at the flame center due to the non-slip condition at the nozzle, they approach uniform velocity distributions immediate downstream of the nozzle exit. This is expected to be due to the influence of buoyancy on the velocity of the fuel flow. Note that the velocities increase gradually with an increase in vertical position z/D, reflecting the contraction effect of the fuel flow as observed in flow visualization picture by tracer injection and reactive Mie scattering method in Figs. 4 and 5, respectively. However, rate of velocity increase is smaller in the case of dilute hydrogen flame due to wider spreading of the fuel jet.

The vertical variations of velocity along the flame axis are shown in Fig. 10 at various CO_2 fractions. The velocity increases with the vertical position z/D from the nozzle exit in most of the flame except near the nozzle exit. With an increase in CO_2 fraction, the vertical velocity decreases gradually due to larger spreading of the fuel jet as observed in Fig. 9.This result is consistent with the reduction of temperature with an increase in CO_2 fraction in Fig. 8, because the vertical velocity is influenced by buoyancy, which is directly proportional to the temperatures. The decrease of 37% in flame temperature results in 32% reduction in velocity along flame axis for $z/D \geq 3$, when CO_2 fraction increases from 0 to 60%. Therefore, the wider spreading of the fuel jet at larger fraction of CO_2 is due to the reduction in temperature. Note that the larger buoyancy is expected in the flame at smaller CO_2 fraction due to the smaller density of the mixture gas. It should be mentioned that the vertical velocity of the fuel jet of pure hydrogen near the nozzle exit shows a large velocity magnitude compared with other cases and this trend is observed in the dilute hydrogen flame of CO_2=20%, too. This peculiar feature of the fuel jet at lower CO_2 concentration can be related to buoyancy of the fuel jet and the corresponding smaller width of the fuel jet near the nozzle exit, but the detail mechanism is not clear.

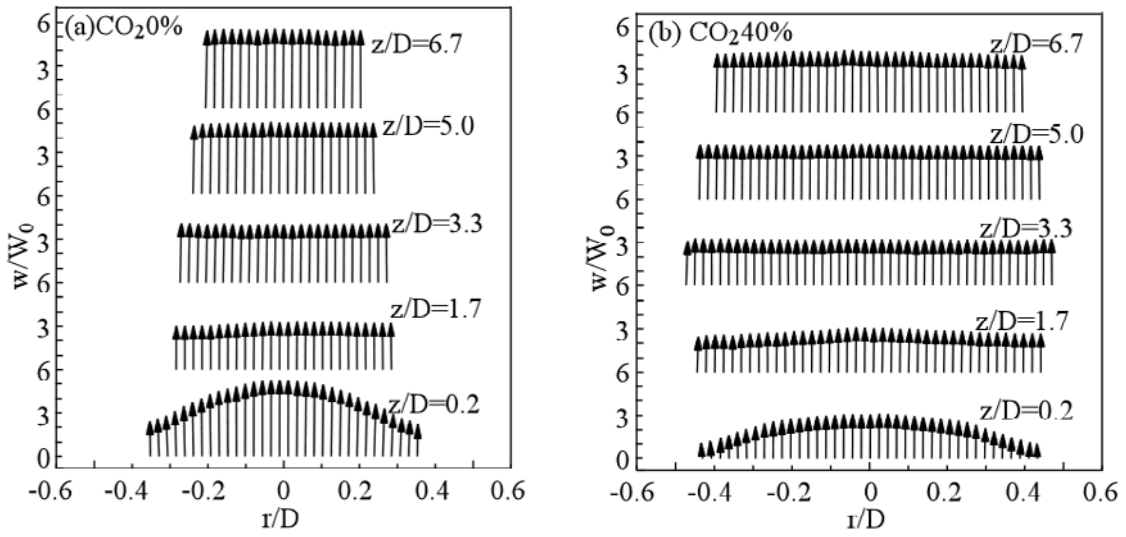

Fig. 9. Velocity distributions.

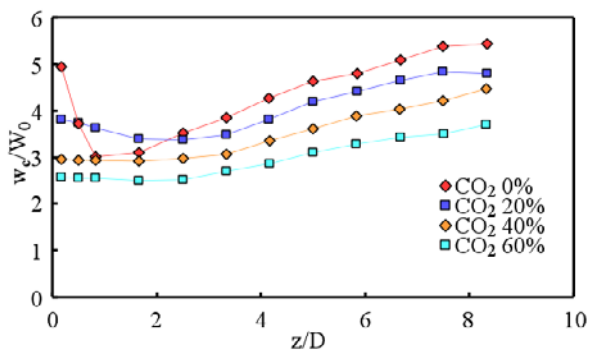

Fig. 10. Variations of velocity along flame axis.

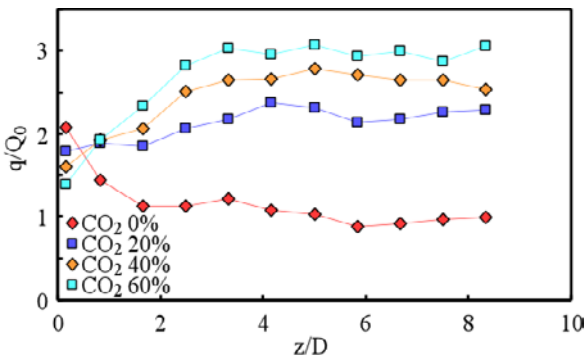

Fig. 11. Variations of flow rate along flame axis.

The local flow rate q of the dilute hydrogen jet is evaluated by integrating the measured velocity field with respect to radial distance r. The result is plotted against the vertical distance z/D, as shown in Fig. 11, where Q_0 is the flow rate measured by the flow meters. It should be mentioned that Q_0 measured by the flow meter agrees with that obtained from PIV with an accuracy of 5% for the non-combusting gases. The local flow rate of pure hydrogen flame decreases suddenly near the nozzle exit due to the influence of chemical reaction in the flame, but it approaches almost constant $q/Q_0 \approx 1$ in further downstream. With an increase in CO_2 fraction in the dilute hydrogen flame, the flow rate increases abruptly near the nozzle exit and stays in a high level ranging from 2 to 3 times that of the pure hydrogen. This result suggests that the entrainment of the surrounding air is greatly increased with an increase in CO_2 fraction, which is due to an increase in density of the mixture gas.

4. Conclusion

The structure of dilute hydrogen flame by CO_2 in air flow is studied by various flow visualization techniques, such as schlieren, direct photograph, tracer injection and reactive Mie scattering method, and the results are compared with the quantitative measurement of temperature and velocity. These results indicate that both the flame temperature and the chemical reaction zone decrease gradually with an increase in CO_2 fraction. Correspondingly, the fuel jet spreads widely and the velocity decreases along the vertical distance with an increase in CO_2 fraction, which results in an increase in flow rate of the fuel jet at larger CO_2 fraction. Therefore, the dilute hydrogen flame becomes more inactive to the chemical reactions at higher CO_2 fraction, which is due to the reduction in buoyancy and the increase in entrainment rate of fuel jet.

Acknowledgement

The authors acknowledge the support from Uchida Energy Science Promotion Foundation.

References

Aung, K. T., Hassan, M. I. and Faeth, G. M., Effects of Pressure and Nitrogen Dilution on Flame/Stretch Interactions of Laminar Premixed $H_2/O_2/N_2$ Flames, Combustion and Flame, 112 (1998), 1-15.

Barlow, R. S., Smith, N. S.A., Chen, J. Y. and Bilger, R. W., Nitric Oxide Formation in Dilute Hydrogen Jet Flames: Isolation of the Effects of Radiation and Turbulence-Chemistry Submodels, Combustion and Flame, 117 (1999), 4-31.

Chen, L.D. and Roquemore, W.M., Visualization of Jet Flames, Combustion and Flames, 66 (1986), 81-86.

Chung, S. H., Several Applications of Laser Diagnostics for Visualization of Combustion Phenomena, Journal of Visualization, 6 (2003), 95-106.

Eickhoff, H. and Winandy, A., Visualization of Vortex Formation in Jet Diffusion Flame, Combustion and Flame, 83 (1991), 263-270.

Feese, J. J. and Turns, S. R., Nitric Oxide Emissions from Laminar Diffusion Flames: Effects of Air-side versus Fuel-side Diluent Addition, Combustion and Flame, 113 (1998), 66-78.

Fiechtner, G. J., Renard, P. H., Carter, C. D., Gord, J. R. and Rolen, J. C., Injection of Single and Multiple Vortices in an Opposed-Jet Burner, Journal of Visualization, 2 (2000), 331-342.

Fujisawa, N., Hosokawa, A. and Tomimatsu, S., Simultaneous Measurement of Droplet Size and Velocity Field by an Interferometric Imaging Technique in Spray Combustion, Measurement Science and Technology, 14 (2003), 1341-1349.

Hargrave, G. K., Williams, T. C. and Jarvis, S., High-speed Visualization of Flame Propagation in Explosions, Journal of Visualization, 4 (2001), 357-364.

Kawanabe, H., Kawasaki, K. and Shioji, M., Gas-flow Measurements in a Jet Flame using Cross-correlation of High-speed-particle Images, Measurement Science and Technology, 11 (2000), 627-632.

Nishimura, T., Kaga, T., Shirotani, K. and Kadowaki, J., Vortex Structures and Temperature Fluctuations in a Bluff-body Burner, Journal of Visualization, 1 (1999), 271-281.

Roquemore, W. M. and Katta, V. R., Role of Flow Visualization in the Development of UNICORN, Journal of Visualization, 2 (2000), 257-272.

Rortveit, G. J., Hustad, J. E., Li, S. C. and Williams, F. A., Effects of Diluents on NOx Formation in Hydrogen Counterflow Flames, Combustion and Flame, 130 (2002), 48-61.

Shioji, M., Yamane, K. Isogami, H. and Ikegami, M., Turbulent Eddies in a Jet Flame as Visualized by a Laser Sheet Method, JSME International Journal, Series B, 36 (1993), 328-334.

Sislian, J. P., Jiang, L. Y. and Cusworth, R. A., Laser Doppler Velocimetry Investigation of the Turbulence Structure of Axisymmetric Diffusion Flames, Prog. Energy Combust. Sci. 14 (1988), 99-146.

Stella, A., Guj, G. and Mataloni, A., Interfrometric Visualization of Jet Flames, Journal of Visualization, 3 (2000), 37-50.

Takagi, T., Komiyama, M., Miyafuji, A. and Yoshida, K., Structure and Dynamic Behavior of Combustion Visualized by 2-D Laser Diagnostics, Journal of Visualization, 2 (2000), 359-370.

Tomimatsu, S., Fujisawa, N. and Hosokawa, A., PIV Measurement of Velocity Field in a Spray Combustor, Journal of Visualization, 6 (2003), 273-281.

Watson, K. A., Lyons, K. M., Donbar, J. M. and Carter, C. D., Visualization of Multiple Scalar and Velocity Fields in a Lifted Jet Flame, Journal of Visualization, 3 (2000), 275-285.

Author Profile

Satoshi Chinone: He was educated at Niigata University (B.E. 2002) and Graduate School of Niigata University (M.E. 2004). He is now working in Japan Defense Agency.

Nobuyuki Fujisawa: After graduating from Tohoku University (D.E. 1983), he joined Gunma University in 1983 and worked as an associate professor since 1991. He has been a professor of Niigata University since 1997. He is interested in visualization, non-intrusive measurement and control of thermal and fluid flow phenomenon in mechanical engineering.